

A Lightweight and Real-Time Binaural Speech Enhancement Model with Spatial Cues Preservation

Jingyuan Wang¹, Jie Zhang¹, Shihao Chen¹, Miao Sun²

¹NERC-SLIP, University of Science and Technology of China (USTC), Hefei, China

²School of Information and Communication Engineering, Guangzhou Maritime University, Guangzhou, China

jywg@mail.ustc.edu.cn; jzhang6@ustc.edu.cn; shchen16@mail.ustc.edu.cn; m.sun.1@hotmail.com

Abstract—Binaural speech enhancement (BSE) aims to jointly improve the speech quality and intelligibility of noisy signals received by hearing devices and preserve the spatial cues of the target for natural listening. Existing methods often suffer from the compromise between noise reduction (NR) capacity and spatial cues preservation (SCP) accuracy and a high computational demand in complex acoustic scenes. In this work, we present a learning-based lightweight binaural complex convolutional network (LBCCN), which excels in NR by filtering low-frequency bands and keeping the rest. Additionally, our approach explicitly incorporates the estimation of interchannel relative acoustic transfer function to ensure the spatial cues fidelity and speech clarity. Results show that the proposed LBCCN can achieve a comparable NR performance to state-of-the-art methods under various noise conditions, but with a much lower computational cost and a better SCP. The reproducible code and audio examples are available at <https://github.com/jywann/LBCCN>.

Index Terms—Binaural noise reduction, spatial cues preservation, lightweight model, relative acoustic transfer function.

I. INTRODUCTION

Speech enhancement (SE) aims to improve the speech quality and intelligibility by reducing background noise, including single-channel and multichannel algorithms, which have developed rapidly over past few decades [1]. For binaural listening devices, e.g., hearing aid (HA), headphone, cochlear implant, which can be used to improve the listening level of hearing-impaired persons, it is expected to not only increase the speech clarity of noisy recordings but also perceive the stereo acoustic scene from the enhanced signals (i.e., spatial awareness). The latter requirement is closely related to binaural cues, which are essential for sound localization [2]. In this sense, conventional SE methods (with a single audio output) usually cannot be directly applied in the binaural context. *The focus of this work is thus on the binaural SE (BSE) with a joint noise reduction (NR) and spatial cues preservation (SCP) of the target speaker.*

Often-used binaural cues include interaural phase difference (IPD), interaural time difference, interaural level difference (ILD), magnitude squared coherence [2]–[4]. Statistical signal processing was initially applied to the BSE task, e.g., minimum variance distortionless response beamformer [5], linearly-constrained minimum variance beamformer [6]–[8], multichannel Wiener filter [9]–[11], [13], parametric unconstrained beamformer [12], by designing two filters at the ears

Financed by the National Natural Science Foundation of China (62101523), Hefei Municipal Natural Science Foundation (2022012) and USTC Research Funds of the Double First-Class Initiative (YD2100002008).

in order to achieve the stereo outputs. These well-established methods can work very well and fast in stationary acoustic conditions, while the efficacy in non-stationary cases is rather limited.

Deep neural network (DNN) is capable of learning a non-linear mapping function from the provided data to the target, which has been widely applied to both single-channel and multichannel SE, even with a better NR performance in non-stationary conditions [14]–[17]. Similarly for BSE, several learning-based methods have been proposed. For instance, in [18] a complex-valued DNN was proposed to suppress interference and preserve the target binaural cues. However, the use of real-valued prediction heads limits the ability to fully exploit the inherent advantages of complex-valued representations. The short-time objective intelligibility (STOI)-optimal masking was adopted in [19], which can enhance the signal-to-noise ratio (SNR) by separately processing the binaural channels, but without a guarantee on the preservation of spatial cues. Further, in [20] two Conv-TasNet [16] networks were configured for binaural channels, which is more promising in performance, while the whole model is computationally intensive and requires substantial memory resources. More recently, the state-of-the-art (SOTA) BSE results can be found in [21], which exploits a complex-valued transformer, yet with a very large model size and high complexity.

As BSE algorithms have to be deployed on latency-sensitive and low-resource listening devices, e.g., HAs, the computationally cheap and low-latency (real-time) models are thus more preferable. To achieve this, we propose a **lightweight binaural complex convolutional network (LBCCN)** for joint binaural NR and SCP. As usually low-frequency signal components can enhance the segregation of competing voices, leading to a better speech understanding in noise [22]–[24], the proposed model selectively filters low-frequency spectrum and keeps the remaining frequencies unchanged. It is shown that this operation can even improve the speech intelligibility at a small sacrifice in the speech quality, but more importantly heavily reduces the computational complexity. The proposed LBCCN leverages pure convolutional network and interchannel relative acoustic transfer function (RATF)-based predictors instead of direct masking [18], [21] to improve the SCP and reduce model parameters. Experimental results on a synthesized dataset demonstrate the superiority of the proposed model in aspects of the BSE performance and computational cost.

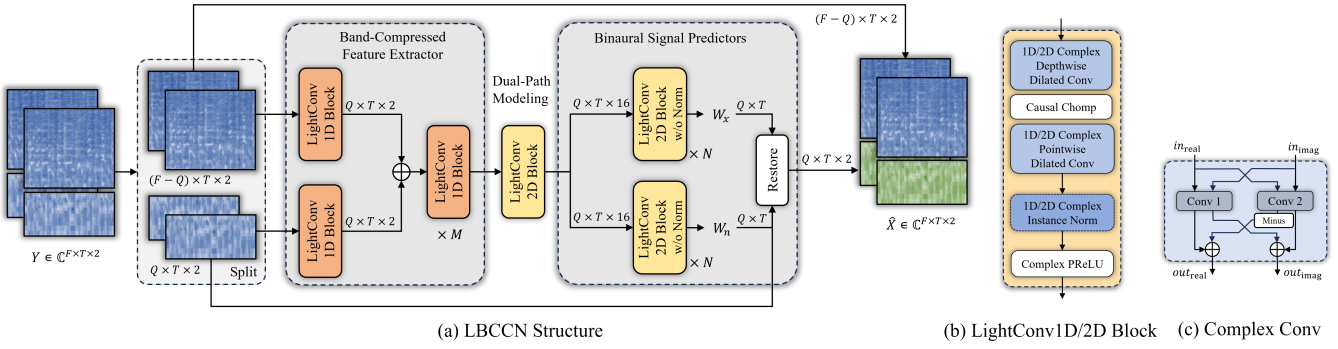


Fig. 1. The proposed LBCCN BSE model, which mainly consists of band-compressed feature extractor (operates on the lower- Q frequency bands), dual-path modeling and signal predictors. The LightConv1D operates on the frequency dimension, and LightConv2D on both time and frequency dimensions.

II. PROPOSED LBCCN METHOD

In the time domain, the binaural signals received by the two ears can be written as

$$\mathbf{y}_i = \mathbf{x}_i + \mathbf{n}_i = \mathbf{h}_i * \mathbf{s} + \mathbf{n}_i, \quad i \in \{L, R\}, \quad (1)$$

where \mathbf{s} represents the original speech signal of interest, \mathbf{x}_i the recorded signal component, \mathbf{n}_i the diffuse isotropic noise component¹, \mathbf{h}_i the head-related impulse responses (HRIRs) of the target speech source with respect to the two ears, $*$ the linear convolution, respectively. The goal of the considered BSE is to extract the target signal components $\mathbf{x}_i, i \in \{L, R\}$ from the received measurements \mathbf{y}_i and preserve the corresponding spatial cues. The proposed LBCCN model mainly consists of the band-compressed feature extractor, dual-path modeling and binaural signal predictors, which is depicted in Fig. 1. Next, we will introduce each module in detail.

A. Band-Compressed Feature Extractor

In order to reduce the computational complexity, we selectively enhance some frequency bands and retain the recorded components in the remaining bands. Our focus is on filtering low-frequency bands, say Q bands, because people perceive the speech signals depending more on low-frequency components, e.g., the fundamental components of vowels, consonants, which are more useful for the segregation of competing voices and speech understanding in noise [22]–[24].

The proposed LBCCN first applies the short-time Fourier transform (STFT) to the input noisy speech signals to obtain time-frequency (TF) representations, followed by two 1D lightweight convolutional (LightConv1D) blocks to compress the frequency spectrum. The LightConv1D blocks are used to process the selected and unselected bands on the frequency dimension, respectively, and their dimensions should adapt to the respective frequency-band numbers. As shown in Fig. 1(b), each LightConv1D block employs a depth-wise separable

¹The spherically diffuse isotropic noise field was shown to be a reasonable approximation of daily practical noise fields in, e.g., an office or car [25]. Given a noise source and HRIRs of all directions, the diffuse isotropic noise component in this work is synthesized by convolving the noise source and each HRIR and then averaging over all convolutions.

causal convolution layer (with depthwise and pointwise convolutions and causal chomp) to ensure the low-complexity and causality. To achieve a larger receptive field, we employ dilated convolutions in these blocks. All operations are complex-valued, such as the complex convolutional layer in Fig. 1(c). These layers are followed by instance normalization and PReLU activation functions. The outputs of these blocks are combined and then processed by M additional LightConv1D blocks for feature extraction. As our focus remains on the low-frequency bands, the compressed latent space dimension is tailored to match that of the low-frequency bands.

B. Dual-Path Modeling

In order to leverage both temporal and frequency speech features for BSE, we employ a 2D lightweight convolutional (LightConv2D) block instead of traditional long short-term memory (LSTM) network [26] or Transformer [27] for dual-path modeling. This design can also reduce the model complexity. The structure of the LightConv2D block is similar to LightConv1D in Fig. 1(b).

C. Binaural Signal Predictors

Existing BSE models usually directly apply estimated masks to predict the binaural outputs [18], [21], given by

$$\hat{\mathbf{X}}_i = \mathbf{M}_i \odot \mathbf{Y}_i, \quad i \in \{L, R\}, \quad (2)$$

where \mathbf{Y}_i and \mathbf{M}_i are the noisy STFT coefficients and complex ideal ratio mask (cIRM) at the two ears, \odot the Hadamard product, respectively. The masks can be seen as the outputs of the LightConv2D blocks in the binaural signal predictors in Fig. 1 and applied to the noisy inputs to recover the target signals via inverse STFT (iSTFT). Hence, the direct masking is a special case of the proposed LBCCN model, referred to as **LBCCN (Masks)** in Section III-B for comparison.

In [28], [29], cascaded binaural speech separation methods were proposed, which first predict the mask for one channel and estimate the RATF. The estimated RATF is then used to calculate the output of the other channel. The inclusion of the RATF estimation is concerned with the preservation of the target binaural cues. It is clear that this cascaded pipeline suffers from the error accumulation, as the overall

signal clarity depends on the RATF accuracy. To show this, we combine the proposed LBCNN backbone with the masking and RATF estimation modules for comparison in Section III-B, referred to as **LBCCN (Mask+RATF)**.

As the binaural cues are closely related to the RATF, in this work we regard the RATF of the target as an implicit prediction target for a better SCP, see the binaural signal predictors in Fig. 1(a). Letting H_L^x and H_R^x denote the ATF of the target source with respect to the two ears, and H_L^n and H_R^n are the average ATF of the noise source in the diffuse isotropic noise field, respectively, we define the frequency-dependent RATFs as $W_x = H_L^x/H_R^x$ and $W_n = H_L^n/H_R^n$. The clean binaural signal components at each TF bin (t, f) can be written as

$$X_L = W_x X_R, \quad X_R = \frac{Y_L - W_n Y_R}{W_x - W_n}, \quad (3)$$

by reformulating the STFT-domain signal model. Unlike the cIRMs M_L and M_R , W_x and W_n have a determined physical meaning. Predicting W_x and W_n directly reflects the SCP and the required number of neurons can be largely reduced, as the number of binaural microphones is usually very small.

We use two prediction heads to estimate the RATFs W_x and W_n in the TF domain, which include N LightConv2D blocks. To alleviate the impact of the amplitude variation on the training stability, we remove the normalization layers in the LightConv2D blocks. After obtaining W_x and W_n , we follow (3) to *Restore* the STFT-domain signal components.

D. Loss Function

Let \hat{x} represent the predicted speech signal, the predicted noise signal \hat{n} is then given by

$$\hat{n} = x + n - \hat{x}. \quad (4)$$

We adopt the weighted signal and noise losses to construct the overall loss function for model training as

$$\mathcal{L}_{\text{total}} = k\mathcal{L}(\hat{x}, x) + (1 - k)\mathcal{L}(\hat{n}, n), \quad (5)$$

where \mathcal{L} is defined similarly as that in [21]:

$$\mathcal{L} = \mathcal{L}_{\text{SNR}} + 10\mathcal{L}_{\text{STOI}} + \mathcal{L}_{\text{IPD}} + 10\mathcal{L}_{\text{ILD}}, \quad (6)$$

which however is calculated over the selected bands. The components in (6) are computed as:

$$\begin{aligned} \mathcal{L}_{\text{SNR}} &= -\frac{1}{2} \sum_{i \in \{L, R\}} 10 \log_{10} \left(\frac{\|x_i\|^2}{\|\hat{x}_i - x_i\|^2} \right), \\ \mathcal{L}_{\text{STOI}} &= -\frac{1}{2} \sum_{i \in \{L, R\}} \text{STOI}(x_i, \hat{x}_i), \\ \mathcal{L}_{\text{ILD}} &= \frac{20}{TF} \sum_t \sum_f \left(\log_{10} \left(\frac{|X_L|}{|X_R|} \right) - \log_{10} \left(\frac{|\hat{X}_L|}{|\hat{X}_R|} \right) \right), \\ \mathcal{L}_{\text{IPD}} &= \frac{1}{TF} \sum_t \sum_f \left(\arctan \left(\frac{|X_L|}{|X_R|} \right) - \arctan \left(\frac{|\hat{X}_L|}{|\hat{X}_R|} \right) \right), \end{aligned}$$

where $\text{STOI}(\cdot)$ represent the short-time objective intelligibility (STOI) measure [30], TF is the total number of TF bins, i.e., the ILD and IPD losses are averaged over all TF bins.

III. EXPERIMENTS

In this section, we will explain the implementation of the proposed LBCNN approach together with the experimental comparison with SOTA models.

A. Experimental Setup

Dataset: To verify the efficacy of the proposed LBCNN model, we create a spatialized anechoic audio dataset, where the clean speech source originates from LibriSpeech [31] and noise source from NoiseX-92 [32]. The HRIRs are derived from the CIPIC [33] dataset, which contains 45 subjects, each measured at 25 azimuth angles (80° to $+80^\circ$) and 50 elevations (90° to $+270^\circ$). Data from 36 subjects are used for training and validation, and the remaining 9 unseen subjects for testing. Clean speech signals are convolved with randomly selected HRIRs to generate the binaural clean signal components, and noise signals are convolved with the HRIRs but averaged over all directions to simulate the isotropic noise components. All datasets is split into training, testing and validation subsets without overlap. The signal and noise components are added together at a random SNR ranging from -10 dB to 10 dB, resulting in 50000 2-seconds samples (≈ 28 hours in total). The samples are divided into at a ratio of 8:1:1 for training, testing and validation, and all are downsampled to 16 kHz.

Training details: We apply a 256-point STFT to the noisy binaural signals using a Hanning window with a hop size of 128, resulting in half-size STFT representations with 129 frequency bins and a maximum frequency of 8kHz. The lowest 40 frequency points are selected for BSE, i.e., $Q = 40$. The weight k in (5) is set to 0.5. The feature extractor has $M = 2$ LightConv1D blocks, and the signal predictor has $N = 3$ LightConv2D blocks. The LightConv blocks have output channels of $\{40, 40, 40, 40\}$, $\{16\}$ and $\{16, 16, 1\}$, kernel sizes of 5, 9 and 9, and dilation rates of $\{1, 1, 2, 4\}$, $\{1\}$ and $\{1, 2, 4\}$ for the band-compressed feature extractor, dual-path modeling and binaural signal predictor, respectively. Padding is applied in each module to keep the output dimensions consistent. The Adam optimizer [34] is used for the training of LBCNN with an initial learning rate of 0.0001, and the model is trained for 20-50 epochs until convergence.

Evaluation metrics: For the comparison of BSE models, we use the modified binaural STOI (MBSTOI) [35] and the gain of perceptual evaluation of speech quality (Δ PESQ) [36] to measure the NR performance (the higher, the better), which are averaged over the two channels. The losses \mathcal{L}_{ILD} and \mathcal{L}_{IPD} (averaged over all TF bins) in Section II-D are used to measure the SCP errors (the lower, the better).

B. Experimental Results

First, we compare the performance of the proposed LBCNN with DBSEnh [18], BiTasNet [20] BCCTN [21]. The comparison models are reproduced strictly according to the published papers. The obtained results are summarized in Table I. Our method achieves the highest speech intelligibility in MBSTOI in all SNR conditions, which is more obvious in more noisy conditions. Meanwhile, the SCP errors of the proposed method

TABLE I
PERFORMANCE COMPARISON OF BSE METHODS IN TERMS OF THE SNR LEVEL.

Input SNR	-10 dB				-5 dB				0 dB			
Method	MBSTOI \uparrow	Δ PESQ \uparrow	\mathcal{L}_{ILD} \downarrow	\mathcal{L}_{IPD} \downarrow	MBSTOI \uparrow	Δ PESQ \uparrow	\mathcal{L}_{ILD} \downarrow	\mathcal{L}_{IPD} \downarrow	MBSTOI \uparrow	Δ PESQ \uparrow	\mathcal{L}_{ILD} \downarrow	\mathcal{L}_{IPD} \downarrow
DBSEnh [18]	0.72	0.01	4.84	0.94	0.80	0.05	4.47	0.80	0.87	0.10	4.04	0.59
BiTasNet [20]	0.80	0.35	5.16	1.05	0.86	0.52	4.53	0.91	0.90	0.71	3.90	0.80
BCCTN [21]	0.81	0.41	3.55	0.83	0.87	0.66	2.99	0.70	0.92	0.97	2.10	0.49
LBCCN	0.88	0.34	3.64	0.68	0.91	0.61	3.14	0.59	0.94	0.87	2.33	0.47
Input SNR	5 dB				10 dB				Average			
Method	MBSTOI \uparrow	Δ PESQ \uparrow	\mathcal{L}_{ILD} \downarrow	\mathcal{L}_{IPD} \downarrow	MBSTOI \uparrow	Δ PESQ \uparrow	\mathcal{L}_{ILD} \downarrow	\mathcal{L}_{IPD} \downarrow	MBSTOI \uparrow	Δ PESQ \uparrow	\mathcal{L}_{ILD} \downarrow	\mathcal{L}_{IPD} \downarrow
DBSEnh [18]	0.91	0.08	3.99	0.50	0.93	0.10	3.98	0.41	0.85	0.06	4.22	0.64
BiTasNet [20]	0.93	0.73	3.58	0.72	0.94	0.72	3.38	0.68	0.89	0.61	4.09	0.83
BCCTN [21]	0.95	1.03	1.63	0.37	0.96	1.07	1.32	0.28	0.90	0.86	2.27	0.58
LBCCN	0.95	1.01	1.97	0.41	0.96	1.01	1.78	0.37	0.93	0.78	2.53	0.50

TABLE II

THE MODEL COMPLEXITY, COMPUTATIONAL REQUIREMENTS AND REAL TIME FACTOR (RTF) OF DIFFERENT BSE METHODS.

Method	Parameters \downarrow	MACs \downarrow	RTF \downarrow
DBSEnh [18]	10.5 M	11.1 G	0.022
BiTasNet [20]	1.7 M	17.2 G	0.329
BCCTN [21]	11.1 M	12.7 G	0.228
LBCCN	38.0 K	216.3 M	0.054

TABLE III

ABLATION STUDY ON BAND COMPRESSION AND SIGNAL PREDICTORS.

Method	MBSTOI \uparrow	Δ PESQ \uparrow	\mathcal{L}_{ILD} \downarrow	\mathcal{L}_{IPD} \downarrow	RTF \downarrow
LBCCN ($Q = 30$)	0.93	0.64	2.41	0.47	0.054
LBCCN ($Q = 40$)	0.93	0.78	2.53	0.50	0.054
LBCCN ($Q = 64$)	0.93	0.69	2.96	0.72	0.057
LBCCN ($Q = 129$)	0.92	0.75	3.48	1.07	0.063
LBCCN (Masks)	0.86	0.17	2.54	0.51	0.054
LBCCN (Mask+RATF)	0.70	0.14	2.44	0.49	0.054
LBCCN (RATFs)	0.93	0.78	2.53	0.50	0.054

are competitive with the BCCTN model, which are lower than the other two methods. It seems that filtering on low-frequency bands (e.g., LBCCN) is more helpful for the preservation of IPD. In Table II, we compare the model size and computational complexity of these approaches, which are calculated using the `thop` package². Clearly, the LBCCN requires significantly less parameters and MACs compared to other methods. Also, the real-time factor (RTF)³ of LBCCN is much smaller than that of BiTasNet and BCCTN and slightly higher than that of DBSEnh. Note that the proposed LBCCN has an obvious superiority in performance over DBSEnh.

Second, we conduct ablation studies on the frequency band selection and signal predictor in Table III. It shows that filtering on the Q selected frequency bands has an impact on both the performance and RTF. In general, the case of $Q = 40$ (i.e., the upper-bound frequency equals $8 \times 40/129 = 2.48$ kHz) returns the best NR performance, which almost covers all important bands for the estimation of speech intelligibility [37], and reducing the selected bands to $Q = 30$ can improve the SCP a bit. On the other side, the RTF increases in terms of Q . Therefore, we choose $Q = 40$ unless stated elsewhere. In addition, the use of signal predictors does not impact the

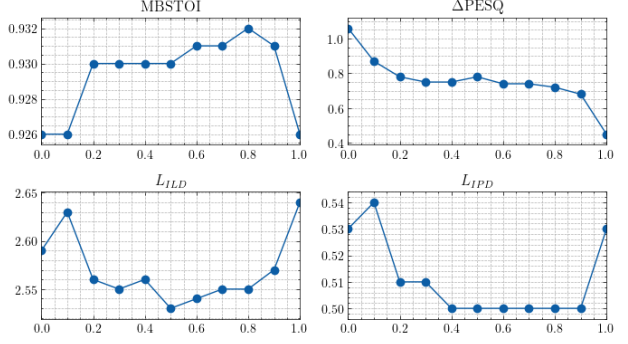


Fig. 2. The impact of the signal and noise losses weight k in (5).

RTF (as the model structures are the same), but influences the performance. The **LBCCN (Masks)** that generates two masks obtains the worst performance. The **LBCCN (Mask+RATF)** that generates a mask and an RATF achieves a better SCP, since estimating a single RATF is easier than estimating two by **LBCCN (RATFs)**. The proposed **LBCCN (RATFs)** that directly outputs two RATFs can significantly increase the NR capacity at the tiny loss in SCP.

Finally, we analyze the impact of the weight parameter k in (5) in Fig. 2, where the performance is averaged over all noise conditions. We observe that the choice of $k = 0.5$ yields the best trade-off between the NR performance and SCP errors, since the average SNR of the considered training set is 0dB. That is, the best balance weight k should depend on the average SNR level of the training samples.

IV. CONCLUSION

In this paper, we proposed a new BSE approach for joint binaural NR and SCP, called LBCCN, which is a lightweight, low-complexity and real-time model. The model complexity was reduced by selectively operating on low-frequency bands that are more related to speech understanding in noise and applying the lightweight convolutional blocks to replace normal convolutions. The binaural cues can be better preserved owing to the inclusion of an explicit estimation of the target RATF. It was shown that the proposed LBCCN can achieve the best performance at most SNR levels, but a more promising superiority in complexity, exhibiting as a more appropriate choice for the deployment on resource-limited listening devices.

²<https://github.com/Lyken17/pytorch-OpCounter>.

³The RTF is measured with Intel(R) Xeon(R) E5-2620 v4 CPU.

REFERENCES

[1] S. Gannot, E. Vincent, S. Markovich-Golan, and A. Ozerov, "A consolidated perspective on multimicrophone speech enhancement and source separation," *IEEE/ACM Trans. Audio, Speech, Lang. Process.*, vol. 25, no. 4, pp. 692–730, 2017.

[2] J. Blauert, *Spatial hearing: the psychophysics of human sound localization*. MIT press, 1997.

[3] T. C. Yin, "Neural mechanisms of encoding binaural localization cues in the auditory brainstem," in *Integrative functions in the mammalian auditory pathway*, pp. 99–159, Springer, 2002.

[4] R. Beutelmann and T. Brand, "Prediction of speech intelligibility in spatial noise and reverberation for normal-hearing and hearing-impaired listeners," *J. Acoust. Soc. Am.*, vol. 120, no. 1, pp. 331–342, 2006.

[5] E. Hadad, D. Marquardt, S. Doclo, and S. Gannot, "Theoretical analysis of binaural transfer function MVDR beamformers with interference cue preservation constraints," *IEEE/ACM Trans. Audio, Speech, Lang. Process.*, vol. 23, no. 12, pp. 2449–2464, 2015.

[6] H. As'ad, M. Bouchard, and H. Kamkar-Parsi, "A robust target linearly constrained minimum variance beamformer with spatial cues preservation for binaural hearing aids," *IEEE/ACM Trans. Audio, Speech, Lang. Process.*, vol. 27, no. 10, pp. 1549–1563, 2019.

[7] E. Hadad, S. Doclo, and S. Gannot, "The binaural LCMV beamformer and its performance analysis," *IEEE/ACM Trans. Audio, Speech, Lang. Process.*, vol. 24, no. 3, pp. 543–558, 2016.

[8] J. Zhang, R. Heusdens, and R. C. Hendriks, "Rate-distributed binaural LCMV beamforming for assistive hearing in wireless acoustic sensor networks," in *IEEE Workshop on Sensor Array and Multichannel Signal Process. (SAM)*, pp. 460–464, IEEE, 2018.

[9] T. Van den Bogaert, J. Wouters, S. Doclo, and M. Moonen, "Binaural cue preservation for hearing aids using an interaural transfer function multichannel Wiener filter," in *Proc. ICASSP*, vol. 4, pp. IV–565, IEEE, 2007.

[10] T. Van den Bogaert, S. Doclo, J. Wouters, and M. Moonen, "Speech enhancement with multichannel Wiener filter techniques in multimicrophone binaural hearing aids," *J. Acoust. Soc. Am.*, vol. 125, no. 1, pp. 360–371, 2009.

[11] S. Thaleiser and G. Enzner, "Binaural-projection multichannel Wiener filter for cue-preserving binaural speech enhancement," *IEEE/ACM Trans. Audio, Speech, Lang. Process.*, 2023.

[12] J. Zhang and G. Zhang, "A parametric unconstrained beamformer based binaural noise reduction for assistive hearing," *IEEE/ACM Trans. Audio, Speech, Lang. Process.*, vol. 30, pp. 292–304, 2021.

[13] J. Zhang and C. Li, "Quantization-aware binaural MWF based noise reduction incorporating external wireless devices," *IEEE/ACM Trans. Audio, Speech, Lang. Process.*, vol. 29, pp. 3118–3131, 2021.

[14] D. Wang and J. Chen, "Supervised speech separation based on deep learning: An overview," *IEEE/ACM Trans. Audio, Speech, Lang. Process.*, vol. 26, no. 10, pp. 1702–1726, 2018.

[15] D. Stoller, S. Ewert, and S. Dixon, "Wave-U-Net: A multi-scale neural network for end-to-end audio source separation," pp. 334–340, 2018.

[16] Y. Luo and N. Mesgarani, "Conv-TasNet: Surpassing ideal time-frequency magnitude masking for speech separation," *IEEE/ACM Trans. Audio, Speech, Lang. Process.*, vol. 27, no. 8, pp. 1256–1266, 2019.

[17] Y. Hu, Y. Liu, S. Lv, M. Xing, S. Zhang, Y. Fu, and et al., "DCCRN: Deep complex convolution recurrent network for phase-aware speech enhancement," in *Proc. Interspeech*, pp. 2472–2476, 2020.

[18] X. Sun, R. Xia, J. Li, and Y. Yan, "A deep learning based binaural speech enhancement approach with spatial cues preservation," in *Proc. ICASSP*, pp. 5766–5770, IEEE, 2019.

[19] V. Tokala, M. Brookes, and P. A. Naylor, "Binaural speech enhancement using STOI-optimal masks," in *Proc. IWAENC*, pp. 1–5, IEEE, 2022.

[20] C. Han, Y. Luo, and N. Mesgarani, "Real-time binaural speech separation with preserved spatial cues," in *Proc. ICASSP*, pp. 6404–6408, IEEE, 2020.

[21] V. Tokala, E. Grinstein, M. Brookes, S. Doclo, J. Jensen, and P. A. Naylor, "Binaural speech enhancement using deep complex convolutional transformer networks," in *Proc. ICASSP*, pp. 681–685, IEEE, 2024.

[22] A. Büchner, M. Schüssler, R. Battmer, T. Stöver, A. Lesinski-Schiedat, and T. Lenarz, "Impact of low-frequency hearing," *Audiology and neurotology*, vol. 14, no. Suppl. 1, pp. 8–13, 2009.

[23] B. W. Hornsby and T. A. Ricketts, "The effects of hearing loss on the contribution of high-and low-frequency speech information to speech understanding," *J. Acoust. Soc. Am.*, vol. 113, no. 3, pp. 1706–1717, 2003.

[24] G. M. Di Liberto, J. A. O'sullivan, and E. C. Lalor, "Low-frequency cortical entrainment to speech reflects phoneme-level processing," *Current Biology*, vol. 25, no. 19, pp. 2457–2465, 2015.

[25] E. A. Habets and S. Gannot, "Generating sensor signals in isotropic noise fields," *J. Acoust. Soc. Am.*, vol. 122, no. 6, pp. 3464–3470, 2007.

[26] X. Le, H. Chen, K. Chen, and J. Lu, "DPCRN: Dual-path convolution recurrent network for single channel speech enhancement," *arXiv preprint arXiv:2107.05429*, 2021.

[27] F. Dang, H. Chen, and P. Zhang, "DPT-FSNet: Dual-path transformer based full-band and sub-band fusion network for speech enhancement," in *Proc. ICASSP*, pp. 6857–6861, IEEE, 2022.

[28] Z. Feng, Y. Tsao, and F. Chen, "Estimation and correction of relative transfer function for binaural speech separation networks to preserve spatial cues," in *Proc. APSIPA ASC*, pp. 1239–1244, IEEE, 2021.

[29] Z. Feng, Y. Tsao, and F. Chen, "Recurrent neural network-based estimation and correction of relative transfer function for preserving spatial cues in speech separation," in *Proc. EUSIPCO*, pp. 155–159, IEEE, 2022.

[30] C. H. Taal, R. C. Hendriks, R. Heusdens, and J. Jensen, "A short-time objective intelligibility measure for time-frequency weighted noisy speech," in *Proc. ICASSP*, pp. 4214–4217, IEEE, 2010.

[31] V. Panayotov, G. Chen, D. Povey, and S. Khudanpur, "Librispeech: an ASR corpus based on public domain audio books," in *Proc. ICASSP*, pp. 5206–5210, IEEE, 2015.

[32] A. Varga and H. J. Steeneken, "Assessment for automatic speech recognition: II. NOISEX-92: A database and an experiment to study the effect of additive noise on speech recognition systems," *Speech communication*, vol. 12, no. 3, pp. 247–251, 1993.

[33] V. R. Algazi, R. O. Duda, D. M. Thompson, and C. Avendano, "The CIPIC HRTF database," in *Proc. WASPAA*, pp. 99–102, IEEE, 2001.

[34] D. P. Kingma, "Adam: A method for stochastic optimization," *arXiv preprint arXiv:1412.6980*, 2014.

[35] A. H. Andersen, J. M. de Haan, Z.-H. Tan, and J. Jensen, "Refinement and validation of the binaural short time objective intelligibility measure for spatially diverse conditions," *Speech Communication*, vol. 102, pp. 1–13, 2018.

[36] A. W. Rix, J. G. Beerends, M. P. Hollier, and A. P. Hekstra, "Perceptual evaluation of speech quality (PESQ)-a new method for speech quality assessment of telephone networks and codecs," in *Proc. ICASSP*, vol. 2, pp. 749–752, IEEE, 2001.

[37] American National Standards Institute (ANSI), "Methods for calculation of the speech intelligibility index," 1997.